Topological superconductivity in planar Josephson junctions: Narrowing down to the nanowire limit

F. Setiawan, Ady Stern, and Erez Berg

Phys. Rev. B **99**, 220506 — Published 25 June 2019

DOI: 10.1103/PhysRevB.99.220506

Topological superconductivity in planar Josephson junctions: Narrowing down to the nanowire limit

F. Setiawan,[1,*] Ady Stern,[2] and Erez Berg[1,2]

[1] *The James Franck Institute and Department of Physics, University of Chicago, Chicago, IL 60637, USA*
[2] *Department of Condensed Matter Physics, Weizmann Institute of Science, Rehovot, Israel 76100*

(Dated: June 10, 2019)

We theoretically study topological planar Josephson junctions (JJs) formed from spin-orbit-coupled two-dimensional electron gases (2DEGs) proximitized by two superconductors and subjected to an in-plane magnetic field $B_\parallel$. Compared to previous studies of topological superconductivity in these junctions, here we consider the case where the superconducting leads are narrower than the superconducting coherence length. In this limit the system may be viewed as a proximitized multiband wire, with an additional knob being the phase difference ϕ between the superconducting leads. A combination of mirror and time-reversal symmetry may put the system into the class BDI. Breaking this symmetry changes the symmetry class to class D. The class D phase diagram depends strongly on $B_\parallel$ and chemical potential, with a weaker dependence on ϕ for JJs with narrower superconducting leads. In contrast, the BDI phase diagram depends strongly on both $B_\parallel$ and ϕ. Interestingly, the BDI phase diagram has a "fan"-shaped region with phase boundaries which move away from $\phi = \pi$ linearly with $B_\parallel$. The number of distinct phases in the fan increases with increasing chemical potential. We study the dependence of the JJ's critical current on $B_\parallel$, and find that minima in the critical current indicate first-order phase transitions in the junction only when the spin-orbit coupling strength is small. In contrast to the case of a JJ with wide leads, in the narrow case these transitions are not accompanied by a change in the JJ's topological index. Our results, calculated using realistic experimental parameters, provide guidelines for present and future searches for topological superconductivity in JJs with narrow leads, and are particularly relevant to recent experiments on InAs 2DEGs proximitized by narrow Al superconducting leads (A. Fornieri *et al.*, Nature **569**, 89 (2019)).

Majorana zero modes (MZMs) [1–9] are not only of fundamental interest but can also be used as the building blocks for a fault tolerant quantum computation [10, 11]. These MZMs exist in the vortex core of two-dimensional (2D) topological superconductors (TSCs) [12, 13] or at the edge of 1D TSCs [14]. The theoretical proposals on TSCs [13–20] have triggered a tremendous amount of experimental effort to realize TSCs in different platforms ranging from 1D nanowire [21–41], topological insulators [42, 43], and ferromagnetic atomic chains [44–47]. Recently, a two-dimensional electron gas (2DEG) with strong spin-orbit coupling (SOC) and proximitized by two spatially separated superconductors (SCs), thus forming a Josephson junction (JJ), was proposed as a new platform to engineer TSC [48, 49]. Compared to the other setups, this system has the advantage of being able to be tuned into TSC by changing not only the strength of the applied magnetic field but also the superconducting phase difference ϕ across the JJ [48, 49]. Recent experiments [50, 51] using this setup have observed some evidence of the Zeeman- and phase-tunable topological superconductivity in form of zero-bias conductance peaks.

In the presence of a symmetry which is a product of the mirror and time-reversal symmetries [48, 49], the topological planar JJ belongs to the symmetry class BDI in the tenfold classification [52, 53], characterized by a $\mathbb{Z}$ topological invariant $Q_\mathbb{Z}$. This invariant corresponds to the number of MZMs at the junction's end. Breaking this symmetry changes the symmetry class to D with a $\mathbb{Z}_2$ index. For JJs with SCs whose width $W_{\rm SC}$ is much larger than the coherence length ξ (as studied in Refs. [48, 49, 54]), the class BDI and D phase diagrams have weak dependence on the chemical potential but depend strongly on both the Zeeman field and ϕ. Moreover, if ϕ is not externally controlled, then as the Zeeman field is varied the system undergoes a first-order topological phase transition (TPT) where the phase of the ground state jumps from $\phi \approx 0$ (trivial) to $\phi \approx \pi$ (topological) or vice versa. This phase jump [48, 55–57] is accompanied by a minimum in the critical current which can be used as an experimental probe for the TPT.

Motivated by recent experiments on InAs 2DEGs proximitized by narrow Al SCs [50], in this Rapid Communcation we study the topological superconductivity in planar JJs with narrow SCs ($W_{\rm SC} < \xi$), see Fig. 1. We further examine the relation between this system and a 1D multiband nanowire TSC [58, 59]. We establish numerically and analytically that the class D phase diagram depends strongly on the in-plane magnetic field $B_\parallel$ applied along the junction, but only weakly on the superconducting phase difference ϕ. This is due to the presence of multiple normal reflections that originate from the interfaces of the SC leads with the vacuum. Furthermore, the normal reflections make the phase diagram more sensitive to the 2DEG chemical potential. In contrast, the BDI phase diagram is strongly dependent on both $B_\parallel$ and ϕ. Crucially, it exhibits a "fan"-shaped region emerging

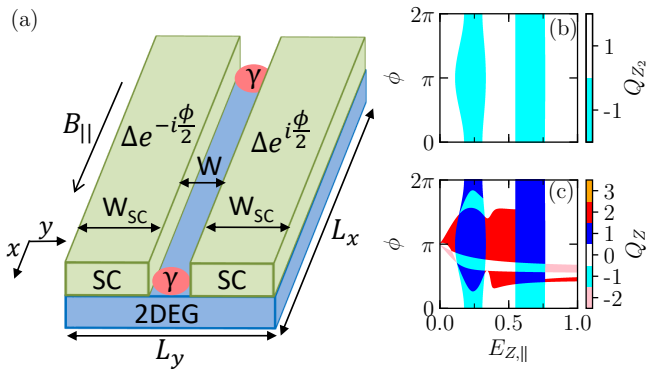

FIG. 1. (a) A JJ made of two narrow SC leads in contact with a 2DEG. By applying an in-plane Zeeman field $E_{Z,||} = g\mu_B B_{||}/2$ parallel to the JJ and a superconducting phase difference ϕ, the system can be tuned into a TSC supporting MZMs γ. (b) Class D and (c) class BDI phase diagrams as functions of $E_{Z,||}$ and ϕ. Regions with odd and even $Q_{\mathbb{Z}}$ topological index in the class BDI [panel (c)] correspond respectively to the topological ($Q_{\mathbb{Z}_2} = -1$) and trivial ($Q_{\mathbb{Z}_2} = 1$) regions of the class D [panel (b)]. The phase diagrams are obtained from numerical simulations performed using the Kwant package [60] of a tight-binding version of Eq. (1) (see Sec. I of Ref. [61]). The parameters used correspond to the experimental parameters of recent experiments on InAs 2DEGs [50], i.e., $m^* = 0.026m_e$, $\alpha = 0.1$ eVÅ, $\mu = 0.6$ meV, $\Delta = 0.15$ meV [$\xi = \hbar v_F/(\pi\Delta) = 126$ nm], $W = 80$ nm, and $W_{\rm SC} = 160$ nm.

from $\phi = \pi$ at $B_{||} = 0$ where the BDI phase boundary lines diverge away from $\phi = \pi$ linearly with $B_{||}$. The number of distinct BDI phases in the fan increases with increasing chemical potential μ as there are more occupied subbands for a larger μ. In addition, the critical current through the junction has minima as a function of $B_{||}$. These minima correspond to discontinuous transitions of the value of ϕ that minimizes the free energy. However, unlike the case of wide SC leads, here these transitions are not necessarily accompanied by a change in the topological index.

The Hamiltonian for the planar JJs [Fig. 1(a)] in the Nambu basis $\Psi_{k_x} = (\psi_{k_x,\uparrow}, \psi_{k_x,\downarrow}, \psi^\dagger_{-k_x,\downarrow}, -\psi^\dagger_{-k_x,\uparrow})^T$ is $H = \frac{1}{2}\int dk_x \int dy \Psi^\dagger_{k_x}(y)\mathcal{H}_{k_x}(y)\Psi_{k_x}(y)$ where

$$\mathcal{H}_{k_x}(y) = \left(\frac{\hbar^2(k_x^2 - \partial_y^2)}{2m^*} - \mu\right)\tau_z + \alpha(k_x\sigma_y + i\partial_y\sigma_x)\tau_z + E_{Z,||}\sigma_x + \Delta(y)\tau_+ + \Delta^*(y)\tau_-, \quad (1)$$

with $\psi_{k_x,\uparrow/\downarrow}(y)$ being the annihilation operator of an electron with spin $\uparrow$ / $\downarrow$ and momentum k_x. Throughout most of this paper, we assume the JJ to be infinitely long. The Pauli matrices $\boldsymbol{\tau}$ and $\boldsymbol{\sigma}$ act in particle-hole and spin spaces, respectively, and $\tau_\pm = (\tau_x \pm i\tau_y)/2$. Here, m^* is the effective electron mass in the 2DEG, μ is the chemical potential, α is the Rashba SOC strength and $E_{Z,||} = g\mu_B B_{||}/2$ is the Zeeman energy due to the applied in-plane magnetic field $B_{||}$. The proximity-induced pairing potential in the 2DEG is [see Fig. 1(a)]

$$\Delta(y) = \begin{cases} \Delta e^{-i\phi/2} & \text{for } -(W_{\rm SC} + W/2) < y < -W/2, \\ 0 & \text{for } -W/2 < y < W/2, \\ \Delta e^{i\phi/2} & \text{for } W/2 < y < W_{\rm SC} + W/2. \end{cases} \quad (2)$$

The Hamiltonian in Eq. (1) anticommutes with the particle-hole operator $P = \sigma_y\tau_y K$ where K denotes complex conjugation. When $E_{Z,||} = 0$ and $\phi = 0$ or π, the Hamiltonian commutes the standard time-reversal operator $T = -i\sigma_y K$ (where $T^2 = -1$) and thus it belongs to the symmetry class DIII [52, 53]. It also commutes with the mirror operator along the x-z plane, i.e., $M_y = -\sigma_y \times (y \to -y)$. While the T and M_y symmetries are broken when $E_{Z,||} \neq 0$ and/or $\phi \neq 0, \pi$, the Hamiltonian remains invariant under the product $\widetilde{T} = M_y T = iK \times (y \to -y)$ [48]. Since $\widetilde{T}^2 = 1$, the system belongs to the class BDI. The presence of $\widetilde{T}$ and P symmetries implies that the Hamiltonian anticommutes with the chirality operator $\widetilde{C} = -iP\widetilde{T} = M_y\tau_y$. Breaking the $\widetilde{T}$ symmetry reduces the symmetry class from BDI to D.

To obtain the phase diagrams, we calculate the topological invariant following Ref. [62]. Since the chirality operator obeys $\widetilde{C}^2 = 1$, it has eigenvalues ± 1. In the basis where $\widetilde{C}$ is diagonal, the Hamiltonian is block off-diagonal (since $\{\widetilde{C}, H\} = 0$). The $\mathbb{Z}$ topological invariant ($Q_{\mathbb{Z}}$) of the class BDI is calculated from the phase of the determinant of the off-diagonal part. The winding of this phase from $k_x = 0$ to $k_x = 2\pi$ gives $Q_{\mathbb{Z}}$. The $\mathbb{Z}_2$ index of class D is simply the parity of $Q_{\mathbb{Z}}$, i.e., $Q_{\mathbb{Z}_2} = (-1)^{Q_{\mathbb{Z}}}$ [14, 62].

Figure 1(b) shows the class D phase diagram of a JJ with narrow leads ($W_{\rm SC} \lesssim \xi$), calculated numerically. The phase diagram shows a sequence of TPTs from the trivial ($Q_{\mathbb{Z}_2} = 1$) to topological ($Q_{\mathbb{Z}_2} = -1$) phases. Contrary to the case of wide SC leads [48], the phase boundaries depend only moderately on ϕ. As $W_{\rm SC}$ becomes smaller, the strength of normal reflections from the SC edges increases resulting in a weaker dependence of the class D phase boundaries on ϕ [63] and the physics crosses over to that of the 1D multiband nanowire TSC [58, 59].

The BDI phase diagram [Fig. 1(c)], on the other hand, depends strongly on both $E_{Z,||}$ and ϕ. For $E_{Z,||} = 0$, the BDI topological invariant is $Q_{\mathbb{Z}} = 0$, except at $\phi = \pi$ where the gap closes. As $E_{Z,||}$ increases, the gap closing point expands into a fan-shaped region containing phases with different values of $Q_{\mathbb{Z}}$.

These features of the phase diagram can be understood qualitatively as follows. Phase transitions where $Q_{\mathbb{Z}_2}$ changes require gap closings at $k_x = 0$, while transitions with an even change in $Q_{\mathbb{Z}}$ occur as a consequence of gap closings at the Fermi wavevector, $k_x = \pm k_F$. In

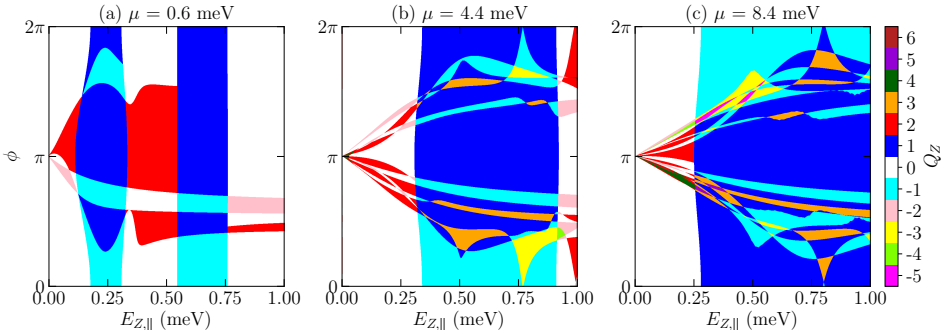

FIG. 2. BDI phase diagrams as functions of Zeeman field $E_{Z,||}$ and superconducting phase difference ϕ for different chemical potentials: (a) $\mu = 0.6$ meV, (b) $\mu = 4.4$ meV, and (c) $\mu = 8.4$ meV. The phase boundary lines inside the "fan"-shaped region emanate from $\phi = \pi$ and $E_{Z,||} = 0$ with slopes which are linearly proportional to $E_{Z,||}$ and decrease with increasing μ. The parameters used are the same as in Fig. 1.

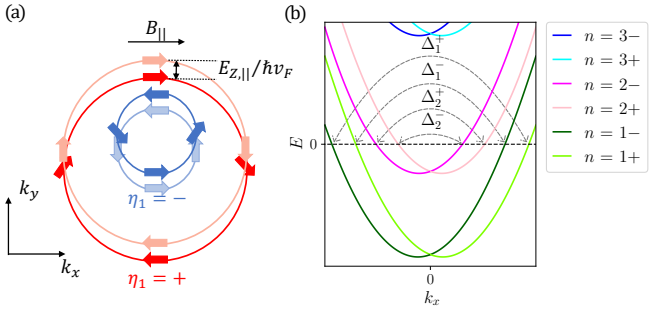

FIG. 3. (a) Fermi surfaces of the 2DEG. An applied magnetic field along x shifts the two spin-orbit split Fermi surfaces (labeled by $\eta_1 = \pm$ for the outer and inner Fermi surface) oppositely along k_y. The arrows show the spin orientation on the Fermi surfaces. The Zeeman field tilts the spin-orientation angle towards its direction. (b) Energy spectrum of an infinitely long 2DEG with a finite width. Each n-th band consists of 2 subbands labeled by $m = \pm$, denoting the eigenvalues of the mirror operator M_y. We label the gap Δ_n^m by the band index n and the mirror eigenvalue $m = \pm 1$ of the right-moving state $k_{F_n} > 0$.

the limit where $\xi \ll W_{\rm SC}$, the system can be treated as a multiband nanowire [58, 59], with an induced gap that is smaller than the energy spacing between subbands. For generic values of μ, the spectrum at $k_x = 0$ is gapped for all ϕ, and therefore the phase diagram depends only weakly on ϕ. This situation changes at special values of μ and $E_{Z,||}$, where the chemical potential enters a new subband (see Sec. II of Ref. [61] for details). Independently of μ, a gap closing occurs at $k_x = \pm k_F$ for $\phi = \pi$ and $E_{Z,||} = 0$. This gap closing occurs as a consequence of the mirror symmetry, where the effective induced gap, which is a spatial average of the gap of two symmetric SC leads, vanishes for $\phi = \pi$ and $E_{Z,||} = 0$.

As shown in Fig. 2, the gap closing point at $\phi = \pi$ and $E_{Z,||} = 0$ expands into a "fan"-shaped region in the phase diagram with phase boundaries which move away from $\phi = \pi$ with slopes which are linearly proportional with $E_{Z,||}$ and decrease with increasing μ. To understand this fan, in the following we derive analytically the dependence of the superconducting gap in a given subband n on $E_{Z,||}$ and ϕ. For simplicity, we work in the limit where $\Delta, E_{Z,||} \ll \alpha k_F \ll \mu$. The dispersion of the 2DEG, shown in Fig. 3(a), exhibits two concentric circular Fermi surfaces. SOC locks the spin orientation to the momentum, such that the outer and inner Fermi surfaces (labeled by $\eta_1 = \pm 1$) have different in-plane spin orientations. When a Zeeman field is applied, the spin tilts towards the Zeeman field direction. Moreover, to the leading order in $E_{Z,||}/(\alpha k_F)$ the Zeeman field also shifts the two Fermi surfaces uniformly along k_y in the opposite direction by $E_{Z,||}/(\hbar v_F)$ [see Fig. 3(a)].

We now take into account the finite size of the system in the y direction. We denote the transverse wavefunctions of the normal Hamiltonian ($\Delta = 0$) by $\varphi^m_{n,k_{F_n},s}(y)$, where n is the band index, $s = \uparrow, \downarrow$, and we label each subband according to the M_y eigenvalue ($m = \pm$) of the state at $k_x = +k_{F_n}$ in the limit $E_{Z,||} = 0$ [see Fig. 3(b)]. A weak Zeeman field mixes the two mirror eigenvalues and opens a gap at $k_x = 0$ but does not strongly affect the wavefunctions at $k_x = k_{F_n}$, such that we may keep using the $\pm$ labeling of the subbands. Te walls at $y = \pm(W/2 + W_{\rm SC})$ mix states with different values of η_1 (See Sec. III of Ref. [61] for the explicit expression of the wavefunction).

Proximitizing the 2DEG with SCs induces intraband pairing potentials $\Delta_n^\pm$ [see Fig. 3(b)]; in the limit $W_{\rm SC} < \xi$, we may neglect the inter-band matrix elements of the pairing potential. The pairing potentials $\Delta_n^\pm$ can be obtained from the first-order degenerate perturbation theory, and are given by (see Sec. IV of Ref. [61])

$$\Delta_n^\pm = \frac{1}{W_{\rm SC} + W/2} \int dy \Delta(y) G_n(y) F_n^\pm(y), \qquad (3)$$

where

$$G_n(y) = \sin^2\left[\frac{n\pi(y + W_{\rm SC} + W/2)}{W_{\rm SC} + W/2}\right], \tag{4a}$$

$$F_n^{\pm}(y) = \varphi^{\pm *}_{n,k_{F_n},\uparrow}(y)\varphi^{\mp *}_{n,-k_{F_n},\downarrow}(y) - (\uparrow\leftrightarrow\downarrow). \tag{4b}$$

To the leading order in Zeeman energy, the intraband pairing potential for the n-th band is

$$\Delta_n^{\pm} = \Delta\frac{W_{\rm SC}}{2W_{\rm SC} + W}\left[(1 + A_n)\cos\left(\frac{\phi}{2}\right) + \frac{E_{Z,||}}{\alpha k_{F_n}}(B_n \pm C_n)\sin\left(\frac{\phi}{2}\right)\right], \tag{5}$$

where A_n is a function of k_{F_n}, W and $W_{\rm SC}$, while B_n and C_n are functions of α, v_{F_n}, k_{F_n}, W and $W_{\rm SC}$ (see Eqs. S-53 and S-54 in Ref. [61]). The zeroth-order term of the gap in the Zeeman energy can be understood intuitively as follows. For JJs with narrow SCs ($W_{\rm SC} \ll \xi$), electrons undergo multiple normal reflections from the edges of the SCs before they can be Andreev reflected. As a result, the gap is the average of the left and right superconducting gaps, i.e., $\Delta_n^{\pm} \propto \Delta(e^{-i\phi/2} + e^{i\phi/2})/2$ which vanishes at $\phi = \pi$. This gap closing also follows from the fact that the Hamiltonian respects the mirror and time-reversal symmetries at $\phi = \pi$ for $E_{Z,||} = 0$ which implies that $F_n^{\pm}(y) = F_n^{\pm}(-y)$ (see Ref. [61] for details). Since $F_n^{\pm}(y)$ and $G_n(y)$ are even functions of y while $\Delta(y)$ is an odd function, $\Delta_n^{\pm} = 0$ at $\phi = \pi$ and $E_{Z,||} = 0$ [see Eq. (3)].

Expanding Eq. (5) around $\phi = \pi$, we have the gap-closing points moving away from $\phi = \pi$ by

$$\delta\phi_n^{\pm} = \frac{2}{(1 + A_n)}\frac{E_{Z,||}}{\alpha k_{F_n}}(B_n \pm C_n). \tag{6}$$

Thus, inside the fan in the BDI phase diagram, the gap closing lines of each subband move away from $\phi = \pi$ with slopes which are inversely proportional to k_{F_n} [see also Fig. 2]. Since these are gap closings at $k_x = \pm k_{F_n}$, they are accompanied by changes in $Q_{\mathbb{Z}}$ by ± 2, but do not affect $Q_{\mathbb{Z}_2}$.

As $E_{Z,||}$ increases, the fan of BDI phase boundaries intersect the class D phase boundary where $Q_{\mathbb{Z}_2}$ changes. As seen in Fig. 2, at each of these intersections, either three or four different phases meet. The four-phase intersection points signify simultaneous gap closings at both $k_x = \pm k_{F_n}$ and $k_x = 0$. The three-phase intersection points happen when two gap closings at $k_x = \pm k_{F_n}$ are moved by varying $E_{Z,||}$ and ϕ, merge at $k_x = 0$, and get lifted (See Sec. V of Ref. [61] for details).

The BDI symmetry can be broken by applying a transverse in-plane magnetic field (along y), disorder that breaks the mirror symmetry, or if the two SCs have different gaps or different widths. Applying a transverse Zeeman field tilts the spectrum, which reduces the gap and results in gapless regions (see Sec. VI A of Ref. [61]). On the other hand, the gap-closing points at $k_x = \pm k_{F_n}$ are lifted when the BDI symmetry is broken by disorder [64] or an asymmetry of the left and right SCs [48, 49, 61]. Breaking the BDI symmetry also results in the hybridization of MZMs residing at the junction's end, leaving either zero or one MZM at each end (see Sec. VI of Ref. [61]). We note that the *exact* BDI symmetry for planar JJs is preserved as long as the left-right symmetry is not broken, independent of the ratio of W and $W_{\rm SC}$ to the spin-orbit length [$\ell_{\rm SO} = \hbar^2/(m^*\alpha)$]. On the other hand, for the case where the left-right symmetry is broken, there is a transition from a class D to an *approximate* BDI symmetry when $W + W_{\rm SC}$ drops below ℓ_{SO}, similar to the nanowire case [62, 65].

Next, we calculate the Josephson current (see Sec. VII of Ref. [61] for details):

$$I(\phi) = \frac{2e}{\hbar}\frac{d\mathcal{F}}{d\phi} = -\frac{4e}{\hbar}\sum_j \tanh\left(\frac{E_j}{2k_{\rm B}T}\right)\frac{dE_j}{d\phi}, \tag{7}$$

where $\mathcal{F}$ is the free energy of the system, T is the temperature, and E_j are the eigenvalues of the Hamiltonian. The critical current is

$$I_c = \max_{\phi} I(\phi). \tag{8}$$

Figure 4 shows I_c and $I(\phi)$ as a function of $E_{Z,||}$ for a JJ with narrow leads at temperature $T = 0.3\Delta/k_{\rm B}$, and for two different values of α. The critical current oscillates as a function of $E_{Z,||}$ with an amplitude that decays with $E_{Z,||}$. For small α, e.g., $\alpha = 0.1$ eVÅ [Figs. 4(a,c)], at the critical Zeeman field where the critical current exhibits a minimum, the phase at which the free energy is minimal changes from $\phi \approx 0$ to $\phi \approx \pi$. Unlike JJs with wide SCs [48], this phase jump does not necessarily imply a TPT due to the weak dependence of the class D TPT on ϕ [Fig. 2(c)]. For larger values of SOC, e.g., $\alpha = 1$ eVÅ [Figs. 4(b,d)], the critical current exhibits a minimum with a shallower depth and at a larger critical Zeeman field. This minimum, however, is not accompanied by a discontinuous change of ϕ that minimizes the free energy. To understand this, we can calculate the energy-phase relation of the junction perturbatively in Δ,

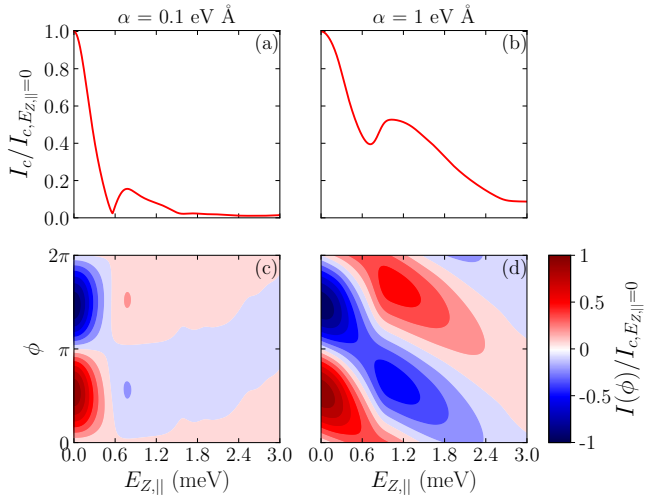

FIG. 4. Upper panel: critical current I_c as a function of Zeeman energy $E_{Z,||}$ for different SOC strengths: (a) $\alpha = 0.1$ eVÅ and (b) $\alpha = 1$ eVÅ. Lower panel: Josephson current as a function of ϕ and $E_{Z,||}$ for (c) $\alpha = 0.1$ eVÅ and (d) $\alpha = 1$ eVÅ. Here, μ is the same as in Fig. 2(c), and the temperature is $T = 0.3\Delta/k_B$. For $\alpha = 0.1$ eVÅ, I_c exhibits a minimum at $E^c_{Z,||} \approx 0.55$ meV. The minimum of the critical current does not coincide with the class D TPT, which occurs at $E_{Z,\|} \approx 0.27$ meV [see Fig. 2(c)]. As α increases, the minimum becomes more shallow [panel (b)]. For small α, there is an abrupt shift by nearly π in the current-phase relation $I(\phi)$ at $E^c_{Z,||}$, while for large α, $I(\phi)$ has a gradual phase shift with $E_{Z,||}$ [see panels (b) and (d), respectively].

for two different limits: $\alpha k_{F_n} \gg E_{Z,||}$ and $\alpha k_{F_n} \ll E_{Z,||}$ (see Sec. VII of Ref. [61]).

In conclusion, we have studied topological superconductivity in planar JJs with narrow SCs and how it crosses over to the nanowire case. As the width of SC leads gets narrower, the strength of normal reflections from the SC edges increases, which renders the class D phase diagram to depend strongly on the chemical potential and more weakly on the superconducting phase difference. On the other hand, the BDI phase diagram is strongly dependent on the superconducting phase difference. Finally, we show that contrary to the wide lead case, the minima in the critical current of JJs with narrow leads do not necessarily indicate TPTs. These results are directly relevant to recent experiments [50], and elucidate the consequences of the BDI symmetry on the phase diagram of these systems.

This work was supported by NSF-DMR-MRSEC 1420709. A. S. and E. B. are supported by CRC 183 of the Deutsche Forschungsgemeinschaft. A.S. acknowledges support from the Israel Science Foundation, the European Research Council (Project LEGOTOP), and Microsoft Station Q.

* setiawan@uchicago.edu

[1] Jason Alicea, "New directions in the pursuit of majorana fermions in solid state systems," Reports on progress in physics **75**, 076501 (2012).
[2] Steven R. Elliott and Marcel Franz, "Colloquium: Majorana fermions in nuclear, particle, and solid-state physics," Rev. Mod. Phys. **87**, 137–163 (2015).
[3] Martin Leijnse and Karsten Flensberg, "Introduction to topological superconductivity and majorana fermions," Semiconductor Science and Technology **27**, 124003 (2012).
[4] C W J Beenakker, "Search for majorana fermions in superconductors," Annu. Rev. Con. Mat. Phys. **4**, 113–136 (2013).
[5] Tudor D Stanescu and Sumanta Tewari, "Majorana fermions in semiconductor nanowires: fundamentals, modeling, and experiment," Journal of Physics: Condensed Matter **25**, 233201 (2013).
[6] Sankar Das Sarma, Michael Freedman, and Chetan Nayak, "Majorana zero modes and topological quantum computation," npj Quantum Information **1**, 15001 (2015).
[7] Carlo Beenakker and Leo Kouwenhoven, "A road to reality with topological superconductors," Nature Physics **12**, 618 (2016).
[8] Ramón Aguado, "Majorana quasiparticles in condensed matter," Riv. Nuovo Cimento **40**, 523–593 (2018).
[9] RM Lutchyn, EPAM Bakkers, LP Kouwenhoven, P Krogstrup, CM Marcus, and Y Oreg, "Majorana zero modes in superconductor–semiconductor heterostructures," Nature Reviews Materials , 1 (2018).
[10] A Yu Kitaev, "Fault-tolerant quantum computation by anyons," Annals of Physics **303**, 2–30 (2003).
[11] Chetan Nayak, Steven H. Simon, Ady Stern, Michael Freedman, and Sankar Das Sarma, "Non-abelian anyons and topological quantum computation," Rev. Mod. Phys. **80**, 1083–1159 (2008).
[12] D. A. Ivanov, "Non-abelian statistics of half-quantum vortices in p-wave superconductors," Phys. Rev. Lett. **86**, 268–271 (2001).
[13] N. Read and Dmitry Green, "Paired states of fermions in two dimensions with breaking of parity and time-reversal symmetries and the fractional quantum hall effect," Phys. Rev. B **61**, 10267–10297 (2000).
[14] A Yu Kitaev, "Unpaired majorana fermions in quantum wires," Physics-Uspekhi **44**, 131 (2001).
[15] Roman M. Lutchyn, Jay D. Sau, and S. Das Sarma, "Majorana fermions and a topological phase transition in semiconductor-superconductor heterostructures," Phys. Rev. Lett. **105**, 077001 (2010).
[16] Yuval Oreg, Gil Refael, and Felix von Oppen, "Helical liquids and majorana bound states in quantum wires," Phys. Rev. Lett. **105**, 177002 (2010).
[17] Liang Fu and C. L. Kane, "Superconducting proximity effect and majorana fermions at the surface of a topological insulator," Phys. Rev. Lett. **100**, 096407 (2008).
[18] T.-P. Choy, J. M. Edge, A. R. Akhmerov, and C. W. J. Beenakker, "Majorana fermions emerging from magnetic nanoparticles on a superconductor without spin-orbit coupling," Phys. Rev. B **84**, 195442 (2011).
[19] S. Nadj-Perge, I. K. Drozdov, B. A. Bernevig, and Ali

Yazdani, "Proposal for realizing majorana fermions in chains of magnetic atoms on a superconductor," Phys. Rev. B **88**, 020407 (2013).
[20] P. M. R. Brydon, S. Das Sarma, Hoi-Yin Hui, and Jay D. Sau, "Topological yu-shiba-rusinov chain from spin-orbit coupling," Phys. Rev. B **91**, 064505 (2015).
[21] V. Mourik, K. Zuo, S. M. Frolov, S. R. Plissard, E. P. A. M. Bakkers, and L. P. Kouwenhoven, "Signatures of majorana fermions in hybrid superconductor-semiconductor nanowire devices," Science **336**, 1003–1007 (2012).
[22] Leonid P Rokhinson, Xinyu Liu, and Jacek K Furdyna, "The fractional ac josephson effect in a semiconductor-superconductor nanowire as a signature of majorana particles," Nat. Phys. **8**, 795–799 (2012).
[23] M. T. Deng, C. L. Yu, G. Y. Huang, M. Larsson, P. Caroff, and H. Q. Xu, "Anomalous zero-bias conductance peak in a," Nano Lett. **12**, 6414–6419 (2012).
[24] Anindya Das, Yuval Ronen, Yonatan Most, Yuval Oreg, Moty Heiblum, and Hadas Shtrikman, "Zero-bias peaks and splitting in an al-inas nanowire topological superconductor as a signature of majorana fermions," Nat. Phys. **8**, 887–895 (2012).
[25] H. O. H. Churchill, V. Fatemi, K. Grove-Rasmussen, M. T. Deng, P. Caroff, H. Q. Xu, and C. M. Marcus, "Superconductor-nanowire devices from tunneling to the multichannel regime: Zero-bias oscillations and magnetoconductance crossover," Phys. Rev. B **87**, 241401 (2013).
[26] A. D. K. Finck, D. J. Van Harlingen, P. K. Mohseni, K. Jung, and X. Li, "Anomalous modulation of a zero-bias peak in a hybrid nanowire-superconductor device," Phys. Rev. Lett. **110**, 126406 (2013).
[27] Sven Marian Albrecht, AP Higginbotham, Morten Madsen, Ferdinand Kuemmeth, Thomas Sand Jespersen, Jesper Nygård, Peter Krogstrup, and CM Marcus, "Exponential protection of zero modes in majorana islands," Nature **531**, 206 (2016).
[28] Önder Gül, Hao Zhang, Jouri DS Bommer, Michiel WA de Moor, Diana Car, Sébastien R Plissard, Erik PAM Bakkers, Attila Geresdi, Kenji Watanabe, Takashi Taniguchi, *et al.*, "Ballistic majorana nanowire devices," Nature nanotechnology **13**, 192 (2018).
[29] Jun Chen, Peng Yu, John Stenger, Moïra Hocevar, Diana Car, Sébastien R Plissard, Erik PAM Bakkers, Tudor D Stanescu, and Sergey M Frolov, "Experimental phase diagram of zero-bias conductance peaks in superconductor/semiconductor nanowire devices," Science advances **3**, e1701476 (2017).
[30] MT Deng, S Vaitiekėnas, Esben Bork Hansen, Jeroen Danon, M Leijnse, Karsten Flensberg, Jesper Nygård, P Krogstrup, and Charles M Marcus, "Majorana bound state in a coupled quantum-dot hybrid-nanowire system," Science **354**, 1557–1562 (2016).
[31] H. J. Suominen, M. Kjaergaard, A. R. Hamilton, J. Shabani, C. J. Palmstrøm, C. M. Marcus, and F. Nichele, "Zero-energy modes from coalescing andreev states in a two-dimensional semiconductor-superconductor hybrid platform," Phys. Rev. Lett. **119**, 176805 (2017).
[32] Fabrizio Nichele, Asbjørn C. C. Drachmann, Alexander M. Whiticar, Eoin C. T. O'Farrell, Henri J. Suominen, Antonio Fornieri, Tian Wang, Geoffrey C. Gardner, Candice Thomas, Anthony T. Hatke, Peter Krogstrup, Michael J. Manfra, Karsten Flensberg, and Charles M. Marcus, "Scaling of majorana zero-bias conductance peaks," Phys. Rev. Lett. **119**, 136803 (2017).
[33] Hao Zhang, Chun-Xiao Liu, Sasa Gazibegovic, Di Xu, John A Logan, Guanzhong Wang, Nick Van Loo, Jouri DS Bommer, Michiel WA De Moor, Diana Car, *et al.*, "Quantized majorana conductance," Nature **556**, 74 (2018).
[34] Hao Zhang, Önder Gül, Sonia Conesa-Boj, Michał P Nowak, Michael Wimmer, Kun Zuo, Vincent Mourik, Folkert K De Vries, Jasper Van Veen, Michiel WA De Moor, *et al.*, "Ballistic superconductivity in semiconductor nanowires," Nature communications **8**, 16025 (2017).
[35] Joachim E. Sestoft, Thomas Kanne, Aske Nørskov Gejl, Merlin von Soosten, Jeremy S. Yodh, Daniel Sherman, Brian Tarasinski, Michael Wimmer, Erik Johnson, Mingtang Deng, Jesper Nygård, Thomas Sand Jespersen, Charles M. Marcus, and Peter Krogstrup, "Engineering hybrid epitaxial inassb/al nanowires for stronger topological protection," Phys. Rev. Materials **2**, 044202 (2018).
[36] M.-T. Deng, S. Vaitiekenas, E. Prada, P. San-Jose, J. Nygård, P. Krogstrup, R. Aguado, and C. M. Marcus, "Nonlocality of majorana modes in hybrid nanowires," Phys. Rev. B **98**, 085125 (2018).
[37] Dominique Laroche, Daniël Bouman, David J van Woerkom, Alex Proutski, Chaitanya Murthy, Dmitry I Pikulin, Chetan Nayak, Ruben JJ van Gulik, Jesper Nygård, Peter Krogstrup, *et al.*, "Observation of the 4π-periodic josephson effect in inas nanowires," Nature Communications **10**, 245 (2019).
[38] Jasper van Veen, Alex Proutski, Torsten Karzig, Dmitry I. Pikulin, Roman M. Lutchyn, Jesper Nygård, Peter Krogstrup, Attila Geresdi, Leo P. Kouwenhoven, and John D. Watson, "Magnetic-field-dependent quasiparticle dynamics of nanowire single-cooper-pair transistors," Phys. Rev. B **98**, 174502 (2018).
[39] Michiel WA de Moor, Jouri DS Bommer, Di Xu, Georg W Winkler, Andrey E Antipov, Arno Bargerbos, Guanzhong Wang, Nick van Loo, Roy LM Veld, Sasa Gazibegovic, *et al.*, "Electric field tunable superconductor-semiconductor coupling in majorana nanowires," New Journal of Physics **20**, 103049 (2018).
[40] Anna Grivnin, Ella Bor, Moty Heiblum, Yuval Oreg, and Hadas Shtrikman, "Concomitant opening of a topological bulk-gap with an emerging majorana edge-state," arXiv preprint arXiv:1807.06632 (2018).
[41] S Vaitiekėnas, M-T Deng, P Krogstrup, and CM Marcus, "Flux-induced majorana modes in full-shell nanowires," arXiv preprint arXiv:1809.05513 (2018).
[42] Jin-Peng Xu, Mei-Xiao Wang, Zhi Long Liu, Jian-Feng Ge, Xiaojun Yang, Canhua Liu, Zhu An Xu, Dandan Guan, Chun Lei Gao, Dong Qian, Ying Liu, Qiang-Hua Wang, Fu-Chun Zhang, Qi-Kun Xue, and Jin-Feng Jia, "Experimental detection of a majorana mode in the core of a magnetic vortex inside a topological insulator-superconductor $bi_2te_3/nbse_2$ heterostructure," Phys. Rev. Lett. **114**, 017001 (2015).
[43] Hao-Hua Sun, Kai-Wen Zhang, Lun-Hui Hu, Chuang Li, Guan-Yong Wang, Hai-Yang Ma, Zhu-An Xu, Chun-Lei Gao, Dan-Dan Guan, Yao-Yi Li, Canhua Liu, Dong Qian, Yi Zhou, Liang Fu, Shao-Chun Li, Fu-Chun Zhang, and Jin-Feng Jia, "Majorana zero mode detected with spin

selective andreev reflection in the vortex of a topological superconductor," Phys. Rev. Lett. **116**, 257003 (2016).
[44] Stevan Nadj-Perge, Ilya K Drozdov, Jian Li, Hua Chen, Sangjun Jeon, Jungpil Seo, Allan H MacDonald, B Andrei Bernevig, and Ali Yazdani, "Observation of majorana fermions in ferromagnetic atomic chains on a superconductor," Science , 1259327 (2014).
[45] Benjamin E Feldman, Mallika T Randeria, Jian Li, Sangjun Jeon, Yonglong Xie, Zhijun Wang, Ilya K Drozdov, B Andrei Bernevig, and Ali Yazdani, "High-resolution studies of the majorana atomic chain platform," Nature Physics **13**, 286 (2017).
[46] Sangjun Jeon, Yonglong Xie, Jian Li, Zhijun Wang, B Andrei Bernevig, and Ali Yazdani, "Distinguishing a majorana zero mode using spin-resolved measurements," Science **358**, 772–776 (2017).
[47] Rémy Pawlak, Marcin Kisiel, Jelena Klinovaja, Tobias Meier, Shigeki Kawai, Thilo Glatzel, Daniel Loss, and Ernst Meyer, "Probing atomic structure and majorana wavefunctions in mono-atomic fe chains on superconducting pb surface," Npj Quantum Information **2**, 16035 (2016).
[48] Falko Pientka, Anna Keselman, Erez Berg, Amir Yacoby, Ady Stern, and Bertrand I. Halperin, "Topological superconductivity in a planar josephson junction," Phys. Rev. X **7**, 021032 (2017).
[49] Michael Hell, Martin Leijnse, and Karsten Flensberg, "Two-dimensional platform for networks of majorana bound states," Phys. Rev. Lett. **118**, 107701 (2017).
[50] Antonio Fornieri, Alexander M Whiticar, F Setiawan, Elías Portolés, Asbjørn CC Drachmann, Anna Keselman, Sergei Gronin, Candice Thomas, Tian Wang, Ray Kallaher, *et al.*, "Evidence of topological superconductivity in planar josephson junctions," Nature **569**, 89 (2019).
[51] Hechen Ren, Falko Pientka, Sean Hart, Andrew T Pierce, Michael Kosowsky, Lukas Lunczer, Raimund Schlereth, Benedikt Scharf, Ewelina M Hankiewicz, Laurens W Molenkamp, *et al.*, "Topological superconductivity in a phase-controlled josephson junction," Nature **569**, 93 (2019).
[52] Shinsei Ryu, Andreas P Schnyder, Akira Furusaki, and Andreas WW Ludwig, "Topological insulators and superconductors: tenfold way and dimensional hierarchy," New Journal of Physics **12**, 065010 (2010).
[53] Alexei Kitaev, "Periodic table for topological insulators and superconductors," in *AIP Conference Proceedings*, Vol. 1134 (AIP, 2009) pp. 22–30.
[54] Dillon T. Liu, Javad Shabani, and Aditi Mitra, "Long-range kitaev chains via planar josephson junctions," Phys. Rev. B **97**, 235114 (2018).
[55] Alexander Zyuzin, Mohammad Alidoust, and Daniel Loss, "Josephson junction through a disordered topological insulator with helical magnetization," Phys. Rev. B **93**, 214502 (2016).
[56] Mohammad Alidoust and Hossein Hamzehpour, "Spontaneous supercurrent and φ_0 phase shift parallel to magnetized topological insulator interfaces," Phys. Rev. B **96**, 165422 (2017).
[57] Mohammad Alidoust, Morten Willatzen, and Antti-Pekka Jauho, "Strain-engineered majorana zero energy modes and φ_0 josephson state in black phosphorus," Phys. Rev. B **98**, 085414 (2018).
[58] Roman M. Lutchyn, Tudor D. Stanescu, and S. Das Sarma, "Search for majorana fermions in multiband semiconducting nanowires," Phys. Rev. Lett. **106**, 127001 (2011).
[59] Tudor D. Stanescu, Roman M. Lutchyn, and S. Das Sarma, "Majorana fermions in semiconductor nanowires," Phys. Rev. B **84**, 144522 (2011).
[60] Christoph W Groth, Michael Wimmer, Anton R Akhmerov, and Xavier Waintal, "Kwant: a software package for quantum transport," New Journal of Physics **16**, 063065 (2014).
[61] See Supplemental Material for (i) details on the tight-binding Hamiltonian, (ii) dependence of class D phase diagrams on the chemical potential and superconducting phase difference, (iii) wavefunction of a Rasbha particle in a strip, (iv) derivation of the dependence of the superconducting gap on the Zeeman energy and superconducting phase difference, (v) explanation of the phase boundaries in the BDI phase diagram, (vi) effects of breaking the BDI symmetry, and (vii) derivation of the Josephson current at zero and finite temperature.
[62] Sumanta Tewari and Jay D. Sau, "Topological invariants for spin-orbit coupled superconductor nanowires," Phys. Rev. Lett. **109**, 150408 (2012).
[63] It was shown recently in Ref. [66] that the chemical potential mismatch between the parent superconductors and 2DEG can also increase the strength of normal reflections which in turn weakens the dependence of the class D phase boundaries on ϕ.
[64] Arbel Haim and Ady Stern, "Benefits of weak disorder in one-dimensional topological superconductors," Phys. Rev. Lett. **122**, 126801 (2019).
[65] M. Diez, J. P. Dahlhaus, M. Wimmer, and C. W. J. Beenakker, "Andreev reflection from a topological superconductor with chiral symmetry," Phys. Rev. B **86**, 094501 (2012).
[66] F. Setiawan, Chien-Te Wu, and K. Levin, "Full proximity treatment of topological superconductors in josephson-junction architectures," Phys. Rev. B **99**, 174511 (2019).